

# Temperature Dependence of the Quasiparticle Excitation Spectrum in $\text{La}_{0.77}\text{Ca}_{0.23}\text{MnO}_3$ films

S. Seiro,\* Y. Fasano, I. Maggio-Aprile, E. Koller, O. Kuffer, and Ø. Fischer

*Département de Physique de la Matière Condensée, Université de Genève,*

*24, Quai Ernest-Ansermet, 1211 Geneva, Switzerland*

(Dated: July 28, 2022)

## Abstract

In this paper the surface quasiparticle excitation spectrum of a single-crystalline fully-strained  $\text{La}_{0.77}\text{Ca}_{0.23}\text{MnO}_3$  film is mapped as a function of temperature using scanning tunneling microscopy. Gapped spectra are found at all temperatures, indicating that polarons are present in both the ‘metallic’ and ‘insulating’ phases. The spatially averaged polaron binding energy presents a sharp minimum in the vicinity of the ‘metal-insulator’ transition temperature but remains finite below. Spectra present sharp band-edge peaks in the ‘metallic’ phase which gradually broaden on warming into the ‘insulating’ phase and pseudogapped spectra are found at room temperature. A conductance gap is detected all over the surface. Therefore there is no coexistence of gapped and ohmic regions at lengthscales greater than  $10 \text{ \AA}$ , in typical fields of view of  $0.1 \mu\text{m}$ . However, local variations in the polaron binding energy of up to 20 % are detected.

PACS numbers: 73.50.-h, 71.30.+h, 68.37.Ef

Keywords: Manganites, Scanning tunneling microscopy, Thin films

---

\*Electronic address: [silvia.seiro@physics.unige.ch](mailto:silvia.seiro@physics.unige.ch)

The complex physics displayed by manganites stems from a subtle balance of competing interactions coupling spin, orbital, charge and lattice degrees of freedom. For certain compounds, a ‘metal’ to ‘insulator’ transition (MIT) occurs on warming through  $T_p$  [1, 2]. Explaining the high-temperature transport properties of manganites required the consideration of the electron-phonon coupling mechanism [3, 4] in addition to double-exchange interactions. In the strong coupling limit, electrons are bound by a surrounding lattice distortion [3, 4], forming polaronic quasiparticles. It is widely accepted that polarons are the charge carriers in the ‘insulating’ phase [5, 6, 7]. However, the nature of the ‘metallic’ phase [8] and the relevance of nanoscale inhomogeneities to the MIT [2] remain active subjects of debate. Insight into this problem can be gained from scanning tunnelling microscopy (STM) studies as the one presented here, which probes electronic properties at the atomic scale.

In the ‘insulating’ phase, polaron hopping was predicted [3, 4] to be the dominant transport mechanism and therefore resistivity becomes thermally activated, as observed experimentally [5, 6, 7]. Within this model, the formation of polarons opens a gap in the quasiparticle spectrum of magnitude  $E_b$ , the binding energy; on cooling below  $T_p$  electron spins order and double exchange becomes dominant, leading to a gapless ‘metallic’ state [3, 4]. However, evidence from numerous experimental techniques suggests the presence of polarons also at  $T < T_p$ , [9, 10, 11, 12] raising the question of the nature of carriers in the ‘metallic’ phase. In particular, optical reflectivity [13] and structural [14, 15] investigations propose a crossover from a large to small-polaron regime on warming across the MIT and a coexistence of both at  $T \sim T_p$ . Other studies also postulate the existence of electronic phase separation, either ‘intrinsic’ or resulting from chemical and crystalline disorder [2].

The phase separation scenario has gained popularity in recent years, although mostly supported by results relying on macroscopic measurements [2]. Few local spectroscopic investigations reported electronic phase separation, but these findings are strongly influenced by chemical, structural or strain inhomogeneities present in the samples [16, 17, 18]. Notably, for the  $\text{La}_{1-x}\text{Ca}_x\text{MnO}_3$  system the coexistence of ‘metallic’ and ‘insulating’ areas in inhomogeneously strained samples was imaged by STM [16], although the absence of phase separation in a fully-relaxed film was recently reported [19].

To shed light into this controversy, the present paper reports a STM investigation on the temperature evolution of the local surface quasiparticle excitation spectrum,  $\rho_s(E, T)$ , of single-crystalline fully-strained  $\text{La}_{0.77}\text{Ca}_{0.23}\text{MnO}_3$  films. Gapped spectra, signature of

polarons with a finite binding energy, are observed both in the ‘metallic’ and ‘insulating’ phases, over the whole field of view. This rules out the coexistence of insulating and fully metallic (ohmic) regions at all measured temperatures. Polaronic quasiparticles present different spectral features below and above  $T_p$ : At low temperatures spectra exhibit sharp band-edge peaks whereas at  $T > T_p$  a gradual broadening of the peaks is detected upon warming. Their absence at 297 K may be associated to a polaron glass-to-liquid transition [7, 20] occurring at a temperature between 176 and 297 K.

Growing  $\text{La}_{0.77}\text{Ca}_{0.23}\text{MnO}_3$  in thin-film form allows to control strain, crystallinity and oxygen content, thereby tuning  $T_p$  and  $E_b$  [21]. Great effort was made to obtain single-crystalline fully-strained samples. The films were grown ex-situ by RF sputtering on (100)  $\text{SrTiO}_3$  at 675°C, in 0.2 Torr of  $\text{Ar}+\text{O}_2$ . Local spectroscopic properties obtained by STM were compared to macroscopic resistivity data. Measurements were performed using a variable temperature home-made STM system [22], which allows to place the sample in ultra-high vacuum prior to cooling in  $^4\text{He}$  exchange gas. Topographs and  $I(V)$  maps were obtained as a function of temperature, with particular detail in the range around  $T_p$ . Optimising the quality of topographs required to change the regulation conditions at each temperature, thereby varying the tunnelling barrier.

The 31 nm-thick film presented in Fig. 1. shows a  $c$  axis parameter of  $(3.808\pm 0.002)$  Å, 1.6% smaller than that of the bulk. The reciprocal space map indicates that the film is fully strained, with 0.9% tensile strain in the  $ab$ -plane and the (103) pole figure shows that the film is single crystalline. Topographs reveal growth steps oriented along the  $\mathbf{a}^*$  and  $\mathbf{b}^*$  axis of the  $\text{La}_{0.77}\text{Ca}_{0.23}\text{MnO}_3$  orthorhombic structure, see Fig. 1 (d). The height of steps is systematically a multiple of  $c$ , the pseudocubic lattice parameter, indicating the same terminating layer over the whole surface. Whether it is  $\text{MnO}_2$  or  $(\text{La,Ca})\text{O}$  planes could not be determined because, although rugosity was on average only 1 Å, atomic resolution [23] was not achieved. Local  $I(V)$  curves were not sensitive to topographic features and rather homogeneous at the nanoscale. Therefore the spatial average is representative of spectroscopic properties over the whole sample surface.

In the STM experimental configuration, if an electron is bound in a polaron, the process of tunnelling into the tip requires the unbinding of the quasiparticle, with an energy cost of  $E_b$ . As a consequence, although the tunnelling particles are electrons, it is possible to evaluate the surface spectrum of the quasiparticles resulting from the unbinding of polarons,

$\rho_s(eV)$ . With this aim,  $10^4$  single  $I(V)$  curves were spatially averaged over  $60 \times 60 \text{ nm}^2$ . At all measured temperatures semiconductor-like behavior was observed and only at 297 K a finite zero-bias conductance was detected, see Figs. 2 (a) and (b).

The surface quasiparticle spectrum can be obtained from  $dI/dV \approx \frac{e^2}{\hbar} \rho_s(eV) \rho_t(0) T(eV, z)$ , where the tip density of states  $\rho_t(0)$  is assumed to be constant and  $z$  is the tip-sample separation [24]. When the tunnel transmission coefficient  $T$  does not depend on  $V$  (for bias voltages much smaller than the barrier height), the measured differential conductance is proportional to  $\rho_s(eV)$ . On the contrary, for semiconductor-like materials the spectral features of interest are detected at voltages comparable to the barrier height so that  $\rho_s(eV) \approx (dI/dV)/T(eV, z)$ . For moderate voltages an adequate estimation of  $T(eV, z)$  is given by  $I/V$  [24]. Considering this, the numerically derived  $I(V)$  curves were normalized to obtain  $\sigma_{\text{norm}} = (dI/dV)/(I/V) \approx \rho_s(eV)$ , the normalized conductance. At energies smaller than the gap the estimation of  $T$  by  $I/V$  is no longer valid because  $I/V$  vanishes while  $T(eV, z)$  must remain finite. In this voltage range,  $T(eV, z)$  was estimated with a WKB-like tunnel transmission coefficient [25]. As a consequence,  $\sigma_{\text{norm}}$  is a measure of the surface quasiparticle excitation spectrum.

To illustrate the evolution of the normalized conductance as a function of temperature, typical spatially-averaged curves obtained in the 31 nm film are presented in Fig. 2. This sample has a MIT at  $T_p = 147 \text{ K}$  and presents thermally activated transport in the ‘insulating’ phase, see insert of Fig. 3. At room temperature  $\sigma_{\text{norm}}$  exhibits a pseudogapped shape; on decreasing temperature within the ‘insulating’ phase a gap opens and broad band-edge peaks develop, consistent with the thermally-activated behaviour of resistivity. At 176 K, a gap  $\Delta = (0.30 \pm 0.07) \text{ eV}$  is found, in agreement with the polaron binding energy  $E_b = (0.22 \pm 0.02) \text{ eV}$  estimated from resistivity. The last value was obtained by fitting the high-temperature resistivity data with a small polaron adiabatic model,  $\rho = \rho_0 T \exp(E_A/kT)$  [5], see Fig. 3. The binding energy can be obtained from  $E_b = 2(E_A - \epsilon_0) = (0.22 \pm 0.02) \text{ eV}$ , where  $\epsilon_0 \sim 10 \text{ meV}$  is the energy necessary to produce a stationary number of carriers [5]. The detection at 297 K of a finite density of states at the Fermi level contrasts the gapped conductance measured at low temperatures. This indicates that a temperature between 176 and 297 K the nature of polarons is changing. Neutron scattering experiments [7, 20] suggest that a freezing from a liquid to a glassy polaronic state with static short-range CE correlations takes place at a temperature  $T^* \lesssim 2T_p$ . Thus,

the 297 K normalized conductance might represent the quasiparticle spectrum of the polaron liquid.

Upon cooling towards the MIT the ‘insulating’ gap narrows and suddenly decreases down to  $(0.14 \pm 0.07)$  eV in a small temperature range close to  $T_p$ . The temperature dependence of  $\Delta$  is shown in Fig. 3. Strikingly, below  $T_p$  the normalized conductance remains gapped and band-edge peaks sharpen, see Fig. 2(d), in apparent contradiction to the temperature evolution of macroscopic resistivity. No local ohmic  $I(V)$  curves were detected in the ‘metallic’ phase, see Fig. 4. However, the resistivity at 4.2 K has a value of  $4 \text{ m}\Omega\text{cm}$ , 3 orders of magnitude larger than for a common metal, consistent with a large effective mass of the charge carriers. A recent angle-resolved photoemission report claims “nodal” quasiparticles near the Fermi level are responsible for ‘metallic’ transport on  $\text{La}_{1.4}\text{Sr}_{1.6}\text{Mn}_2\text{O}_7$  [8]. No signature of a quasiparticle peak near the Fermi energy was found in  $\sigma_{\text{norm}}(V)$ , but considering the tunnelling-current noise in our measurements ( $10^{-2}$  pA) the presence of this peak in  $\text{La}_{0.77}\text{Ca}_{0.23}\text{MnO}_3$  cannot be totally ruled out. Previous STM measurements have also detected a semiconducting-like spectrum at 77 K (‘metallic’ phase) in a  $\text{La}_{0.7}\text{Ca}_{0.3}\text{MnO}_3$  film [26], and a gap at low temperatures on cleaved  $\text{La}_{1.4}\text{Sr}_{1.6}\text{Mn}_2\text{O}_7$  [27]. Furthermore, the sensitivity of  $\Delta(T)$  to the MIT and its quantitative agreement with  $E_b$  in the ‘insulating’ phase, indicate that, although probing the quasiparticle spectrum at the surface, the STM results are representative of bulk properties.

The temperature evolution of  $\sigma_{\text{norm}}$  indicates that polarons in the ‘insulating’ and the ‘metallic’ phase present different spectral features. In the latter case, the sharpness of band-edge peaks, signature of a well-defined binding energy, suggests that polarons order in a coherent state. The temperature dependence of the gap in the ‘metallic’ phase is consistent with polaron binding energies obtained from macroscopic optical reflectivity data [28]. The gradual broadening of the peaks on increasing temperature in the ‘insulating’ phase indicates that polarons start to lose coherence above  $T_p$  and eventually melt at  $T^*$  [7, 20]. These results indicate that  $T_p$  is not the temperature scale controlling the appearance of band-edge peaks. These findings suggest a similarity between spectroscopic properties of manganites and high-temperature superconductors that should be considered in explaining the physics of the transition-metal-oxide family.

Thin films as the one studied here are ideal systems to investigate electronic phase separation in the absence of chemical and crystalline inhomogeneities. Figure 4 shows maps of local

gap values for temperatures close to the MIT, where phase separation would be most likely. Within the experimental resolution ( $\sim 0.03$  eV), a gap is detected everywhere, indicating that a phase separation between ‘metallic’ (ohmic) and ‘insulating’ domains does not occur at length scales greater than  $10 \text{ \AA}$ . The gap value distributions are Gaussian with a dispersion of up to 20% which does not significantly change with temperature (it varies only 2.5% from 176 to 140 K). Furthermore, no bimodal distribution of  $\Delta$  is detected within 0.03 eV, suggesting that a ‘soft’ phase separation in domains with different gaps is not likely. These results imply that ‘intrinsic’ nanoscopic electronic disorder is not relevant to the physics of homogeneous  $\text{La}_{0.77}\text{Ca}_{0.23}\text{MnO}_3$  films. However, our measurements cannot rule out phase separation scenarios concerning orbital or magnetic degrees of freedom.

In summary, three temperature regimes have been identified in the polaronic surface quasiparticle spectrum of single-crystalline fully-strained  $\text{La}_{0.77}\text{Ca}_{0.23}\text{MnO}_3$ . The first tunneling spectroscopic evidence for the existence of coherent polarons in the ‘metallic’ phase, which gradually lose coherence when warming into the ‘insulating’ state, is presented. Pseudogapped spectra detected at room temperature may be associated to the reported high-temperature polaron liquid phase [7, 20]. These novel results bring forth the challenge of understanding the nature of the low-temperature coherent polaronic quasiparticles and their role in the transport mechanisms of manganites.

### Acknowledgments

This work was supported by the Swiss National Science Foundation and the MaNEP program of the Swiss National Center of Competence in Research.

- 
- [1] *Colossal magnetoresistive oxides*, edited by Y. Tokura, Advances in Condensed Matter Science Vol. 2 (Gordon and Breach, Amsterdam, 2000).
  - [2] E. Dagotto, *Nanoscale Phase Separation and Colossal Magnetoresistance* (Springer-Verlag, Berlin, 2003).
  - [3] A. J. Millis, P. B. Littlewood, and B. I. Shraiman, Phys. Rev. Lett. **74**, 5144 (1995).
  - [4] A. J. Millis, B. I. Shraiman, and R. Mueller, Phys. Rev. Lett. **77**, 175 (1996).
  - [5] D. C. Worledge *et al.*, J. Appl. Phys. **80**, 5158 (1996).

- [6] M. Jaime *et al.*, Phys. Rev. B **54**, 11914 (1996).
- [7] J. M. De Teresa *et al.*, Nature **386**, 256 (1997).
- [8] N. Mannella *et al.*, Nature **438**, 474 (2005).
- [9] M. F. Hundley *et al.*, Appl. Phys. Lett. **67**, 860 (1995).
- [10] A. S. Alexandrov *et al.*, Phys. Rev. B **64**, 140404 (2001).
- [11] G.-M. Zhao, V. Smolyaninova, W. Prellier, and H. Keller, Phys. Rev. Lett. **84**, 6086 (2000).
- [12] M. Quijada *et al.*, Phys. Rev. B **58**, 16093 (1998).
- [13] S. Yoon *et al.*, Phys. Rev. B **58**, 2795 (1998).
- [14] D. Louca *et al.*, Phys. Rev. B **56**, R8475 (1997).
- [15] A. Lanzara *et al.*, Phys. Rev. Lett. **81**, 878 (1997).
- [16] M. F  th *et al.*, Science **285**, 1540 (1999). Sample characterization is described in S. Freisem *et al.*, J. Magn. Magn. Mater. **165**, 380 (1997).
- [17] T. Becker *et al.*, Phys. Rev. Lett. **89**, 237203 (2002).
- [18] S. F. Chen *et al.*, Appl. Phys. Lett. **82**, 1242 (2003).
- [19] J. Mitra *et al.*, Phys. Rev. B **71**, 094426 (2005).
- [20] D. N. Argyriou *et al.*, Phys. Rev. Lett. **89**, 036401 (2002).
- [21] X. F. Song, G. J. Lian and G. C. Xiong, Phys. Rev. B **71**, 214427 (2005).
- [22] A. D. Kent *et al.*, Ultramicroscopy **42-44**, 1632 (1992).
- [23] To our knowledge, atomic resolution on manganite films has only been recently achieved and reported in J. X. Ma, D. T. Gillaspie, E. W. Plummer, and J. Shen, Phys. Rev. Lett. **95**, 237210 (2005).
- [24] P. M  rtensson and R. M. Feenstra, Phys. Rev. B. **39**, 7744 (1989).
- [25] V. A. Ukraintsev, Phys. Rev. B. **53**, 11176 (1996).
- [26] J. Y. T. Wei, N. C. Yeh, and R. P. Vasquez, Phys. Rev. Lett. **79**, 5150 (1997).
- [27] H. M. R  nnow *et al.*, Nature **440**, 1025 (2006).
- [28] C. Hartinger, *et al.*, Phys. Rev. B **69**, 100403 (2004).

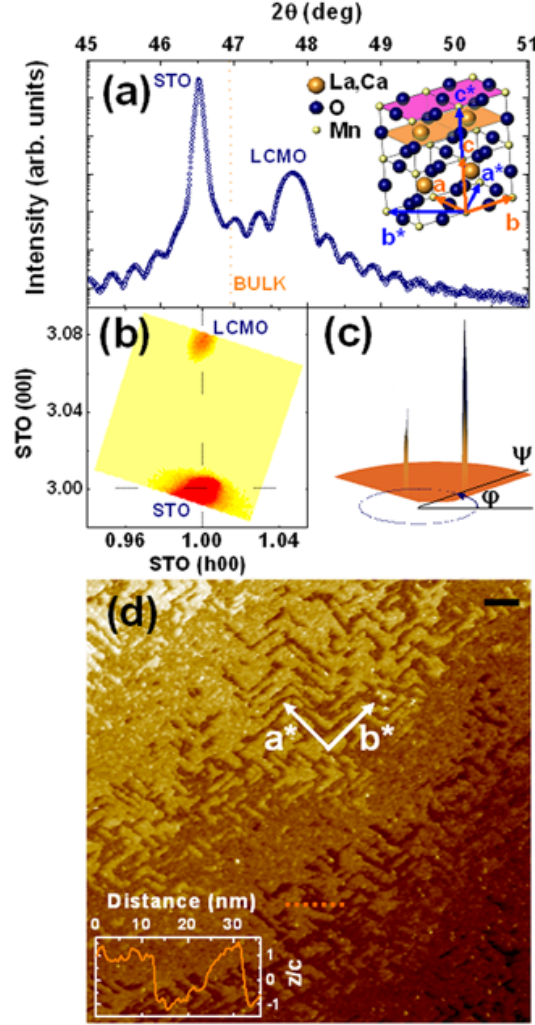


FIG. 1: (a) Main panel: X-ray diffractogram around the (002) pseudocubic reflection and size-effect oscillations. The film thickness was inferred to be 31 nm and the  $c$  axis parameter  $(3.808 \pm 0.002)$  Å. Inset: Schematic crystalline structure. Pseudocubic ( $\mathbf{a}$ ,  $\mathbf{b}$ ,  $\mathbf{c}$ ) and orthorhombic ( $\mathbf{a}^*$ ,  $\mathbf{b}^*$ ,  $\mathbf{c}^*$ ) lattice vectors are indicated, as well as  $\text{MnO}_2$  (pink) and  $(\text{La,Ca})\text{O}$  (orange) planes. (b) Reciprocal space map around the (103) reflection. (c) Pole-figure measurement for the (103) direction. (d) Topograph measured in the constant-current mode with regulation conditions of 2 V and 0.4 nA at 144 K. The  $\mathbf{a}^*$  and  $\mathbf{b}^*$  vectors of the film are at  $45^\circ$  to the  $\mathbf{a}$  and  $\mathbf{b}$  axes of the substrate. The black scale bar represents 20 nm. The height profile in the insert corresponds to the dotted line (orange).

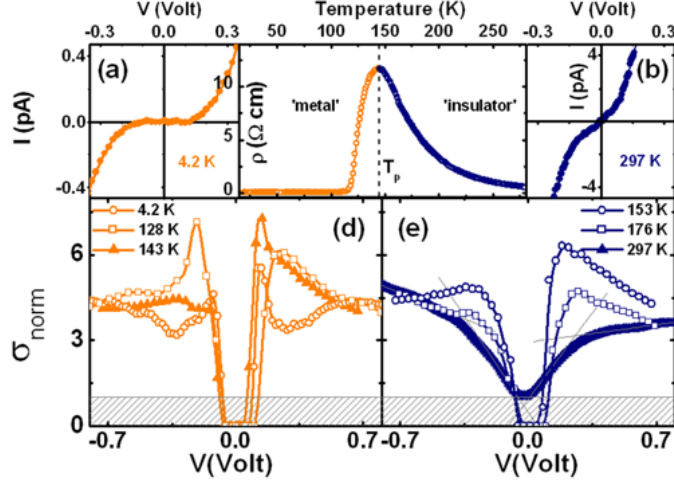


FIG. 2: Average tunneling  $I(V)$  curves for (a) 4.2 K (2 V/0.5 nA) and (b) 297 K (1 V/1 nA).  $I(V)$  curves were measured with the tip (chemically-etched Ir) grounded and a bias voltage applied to the sample. (c) The ‘metal-insulator’ transition temperature is detected in macroscopic resistivity measurements at  $T_p=147$  K (dotted line) with an imprecision of 4 K that arises from measuring at a finite temperature sweep rate. (d) and (e) Selected normalized conductance curves at temperatures below and above  $T_p$ , respectively. When the measured average current was below the experimental noise ( $\sim 10^{-2}$  pA)  $\sigma_{\text{norm}}$  was considered to be zero (hatched regions).

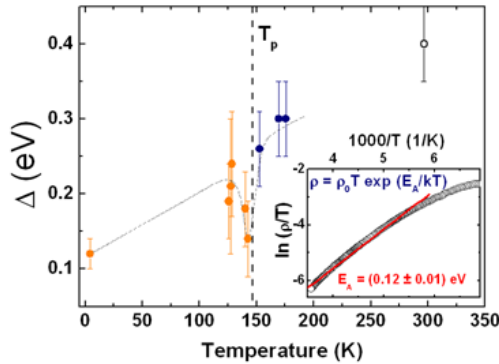


FIG. 3: Temperature dependence of the polaronic gap, estimated from normalized conductance curves as half the peak-to-peak separation in energy (full circles). The open circle indicates the ‘pseudogap’ value estimated from the  $\sigma_{\text{norm}}$  curve measured at 297 K that presents no peaks, obtained as the voltage where the extrapolation of linear fits at low and high voltages cross (see Fig. 2(e)). The dotted line is a guide to the eye. Insert: Fit (red line) of the high-temperature resistivity data (open symbols) with a small polaron adiabatic model.

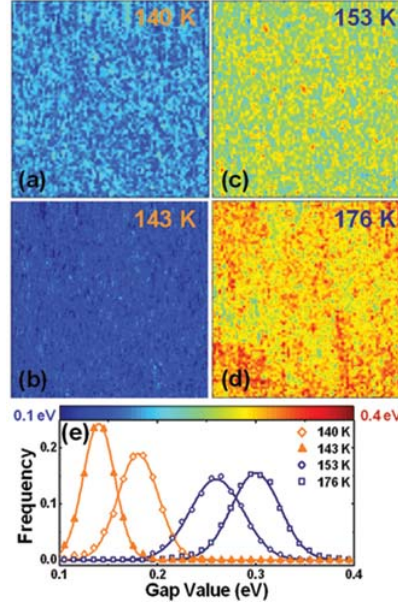


FIG. 4: Mapping of local gap values at (a) 140, (b) 143, (c) 153 and (d) 176 K. All maps correspond to  $60 \times 60 \text{ nm}^2$  areas with a resolution of  $7.5 \text{ \AA}/\text{pixel}$ . (e) Distributions of gap values (symbols) obtained from the maps fitted with a Gaussian law (lines). The average noise of local  $I(V)$  curves in all maps is comparable, ranging from 0.2 to 0.4 pA.